Energy-Efficient Resource Allocation for UAV-Enabled Information and Power Transfer with NOMA

Saif Najmeddin*§, Sonia Aïssa§, Sofiène Tahar*
*Electrical and Computer Engineering, Concordia University, Montreal, Canada
§Institut National de La Recherche Scientifique (INRS-EMT), University of Quebec, Montreal, Canada
Email: s_najmed@ece.concordia.ca, aissa@emt.inrs.ca, tahar@ece.concordia.ca

GLOBECOM 2020 - 2020 IEEE Global Communications Conference | 978-1-7281-8298-8/20/$31.00 ©2020 IEEE | DOI: 10.1109/GLOBECOM42002.2020.9348068

***Abstract*—This paper investigates the energy efficiency optimization in a wireless communication network in which an unmanned aerial vehicle (UAV) deploys information and power transfer towards co-located information and energy receivers to enable downlink and uplink data transmission through non-orthogonal multiple access (NOMA). Using a constructed closed-form expression for the energy efficiency, a resource allocation mechanism aiming at maximizing the energy efficiency of the system is developed. To this end, an algorithm which jointly takes into account the downlink and uplink stages is proposed, using Lagrangian optimization and gradient decent methods. Numerical results and comparisons are provided. In particular, the results show an enhancement in energy efficiency for the NOMA scheme compared with OMA, and that less wireless power transfer time will be needed from the UAV to simultaneously charge energy receivers when using NOMA.**

***Index Terms*—Energy Harvesting; Energy Efficiency; Wireless Power Transfer; UAV; NOMA; WIPT.**

I. Introduction

Among the wide range of applications enabled by unmanned aerial vehicles (UAVs), one of the most important is in Internet of Things (IoT) networks, in which devices have limited power resources and may not be able to communicate over long ranges [1]. With additional flexibility, including 3D mobility and line-of-sight (LoS), UAVs can be efficiently used as wireless power transmitters for battery-limited or hard to reach devices, to enable their data communications [2], while improving the wireless charging efficiency compared to ground power beacons at fixed locations and providing cost-effective on-demand wireless power [3].

In many use-cases, UAVs are called to not only chrge devices, but also to send and/or collect information to/from them [4]. Using the concept of wireless power and information transfer (WIPT) or simultaneous WIPT, where the transmitter sends power and information signals towards energy receivers (ERs) and information receivers (IRs), UAVs can be deployed to provide efficient wireless power transfer (WPT) along with reliable data services when and where needed. The use of such concept needs to meet the radio resource sharing of B5G, where non-orthogonal multiple access (NOMA) will highly likely be replacing the conventional orthogonal multiple access (OMA) [5].

Recently, NOMA received significant attention for its promising performance, despite the additional complexity due the required successive interference cancellation (SIC) [6]. For reliable downlink and uplink NOMA systems, SIC is performed. In the downlink, the user with strong channel condition receives NOMA signal, decodes the symbol of higher power from the received signal, and then subtracts it from the received signal to decode its own symbol [7]. In uplink NOMA, the messages from different users are combined together, and SIC is conducted at the receiver [8].

So far, several research works focused on the resource allocation to enhance the performance of UAV-enabled power or information networks. For instance, the work in [9] suggests a design based on the optimization of UAV's trajectory to enhance throughput while taking into consideration the energy consumption of the UAV and trying to maximize the amount of energy transferred to the ground devices. Leveraging the benefits of NOMA over OMA, the authors in [8] proposed a cooperative NOMA scheme to maximize the weighted sum-rate of the UAV and ground nodes through optimizing the power allocation and the UAV's rate. In [4], joint optimization of the power allocation and trajectory design of the UAV to support infrastructure-starved IoT services was investigated. Besides, minimization of the energy consumption of mobile nodes with acceptable quality-of-service (QoS) has been analyzed in [10], where offloading is enabled by uplink and downlink communications between the nodes and the UAV via NOMA or OMA protocols.

In this work, we address the optimization of the energy efficiency (EE) of a system in which a multi-antenna UAV serves as power and information access point for ground ERs and IRs, where energy harvested by the ERs is used for their uplink NOMA communications towards the same UAV while downlink NOMA transmissions towards IRs are taking place. The portions of power dedicated to ERs and IRs are determined. Moreover, a time allocation scheme is enabled to specify the optimal switching between the energy and information transmissions. Considering constraints on the main system parameters, including the required QoS of the ERs and IRS, and the downlink and uplink thresholds to enable SIC, maximization of the system EE is conducted by optimizing the transmit powers towards the co-existing devices, along with the wireless power charging time of the ERs. Simulation results are provided to illustrate the performance of the NOMA based system in comparison with OMA.

The rest of the paper is organized as follows: Section II describes the system model. Formulation of the EE is detailed

in Section III. The optimization problem is formulated and solved in Section IV. Numerical results are discussed in Section V, and Section VI concludes the paper.

Notation: Symbol $\mathbb{E}\{.\}$ is used for the expectation, $(.)^\dagger$ denotes the Hermitian transpose, and $(.)^H$ indicates the conjugate transpose. Symbol $\|.\|$ denotes the Euclidian norm, and $[.]^+$ refers to $\max(0,.)$.

II. System and Channel Models

The UAV serves K single-antenna IRs and J single-antenna ERs in each time slot T (Fig. 1). The total number of antennas at the UAV is $N = N_E + N_I$, with N_E used for the ERs, and N_I dedicated to the IRs. The time slot is divided into two phases. In the first phase, αT $(0 < \alpha < 1)$, the UAV transmits energy signals to the ERs. In the second phase, $(1-\alpha)T$, the ERs make use of the harvested energy to transmit their always-available data to the UAV. Simultaneously, the UAV transmits information to the IRs. The data transmissions on the uplink (U) and downlink (D) are performed according to the NOMA protocol. Without loss of generality, the time slot duration T is set to unity. The position of the UAV is denoted $(X_{\rm UAV}, Y_{\rm UAV}, h_{\rm UAV})$, the one of ER_j is $(X_{\text{ER}_j}, Y_{\text{ER}_j}, h_{\text{ER}_j})$, and that of IR_k is $(X_{\text{IR}_k}, Y_{\text{IR}_k}, h_{\text{IR}_k})$. In this work, we focus on the system operation once the UAV starts hovering in a specific position, i.e., $(X_{\rm UAV}, Y_{\rm UAV}, h_{\rm UAV})$, for serving the ground devices.

A. Channel Models

Channels are of two types: air-to-ground (A2G) from the UAV to IRs and ERs, and ground-to-air (G2A) from ERs to the UAV. The complex channel vector of link UAV-IR_k is denoted $\mathbf{h}_k \in \mathbb{C}^{1\times N_I}$, $k = 1, \cdots, K$. For ER_j, $j = 1, \cdots, J$, the complex channel vector of the A2G link is denoted $\mathbf{g}_j \in \mathbb{C}^{1\times N_E}$, and the one of the G2A is $\mathbf{z}_j \in \mathbb{C}^{N_E\times 1}$. First, we have $\mathbf{g}_j = \mathbf{g}'_j/\sqrt{L^{\rm D}_{\text{ER}_j}}$, where $L^{\rm D}_{\text{ER}_j}$ is the average path-loss, and $\mathbf{g}'_j = [g'_{j,1}, g'_{j,2}, \ldots, g'_{j,N_E}]$ is the normalized channel fading vector. Assuming Rician fading, $\mathbf{g}'_j$ can be written as [3]:

$$\mathbf{g}_j{}' = \sqrt{\frac{\mathcal{K}}{\mathcal{K}+1}}\mathbf{1}_{1\times N_E} + \sqrt{\frac{1}{\mathcal{K}+1}}\tilde{\mathbf{g}}_j, \tag{1}$$

where $\mathcal{K}$ is the Rice factor, $\mathbf{1}_{1\times N_E}$ is a unity row vector, and the non-line-of-sight (NLoS) fading component $\tilde{\mathbf{g}}_j$ is a row vector whose elements are i.i.d. complex Gaussian random variables with zero mean and unit variance, i.e., $\mathcal{CN}(0,1)$. The average A2G free-space distance-dependent path loss of ER_j, $L^{\rm D}_{\text{ER}_j}$ in dB, is given by

$$L^{\rm D}_{\text{ER}_j} = p_{\text{LoS},j}\, L_{\text{LoS},j} + (1 - p_{\text{LoS},j})\, L_{\text{NLoS},j}, \tag{2}$$

where the LoS and NLoS path losses are given by

$$L_{\text{LoS},j} = 20\log_{10}\left(\frac{4\pi f d_j}{c}\right) + \xi_{\text{LoS},j}, \tag{3}$$

$$L_{\text{NLoS},j} = 20\log_{10}\left(\frac{4\pi f d_j}{c}\right) + \xi_{\text{NLoS},j}, \tag{4}$$

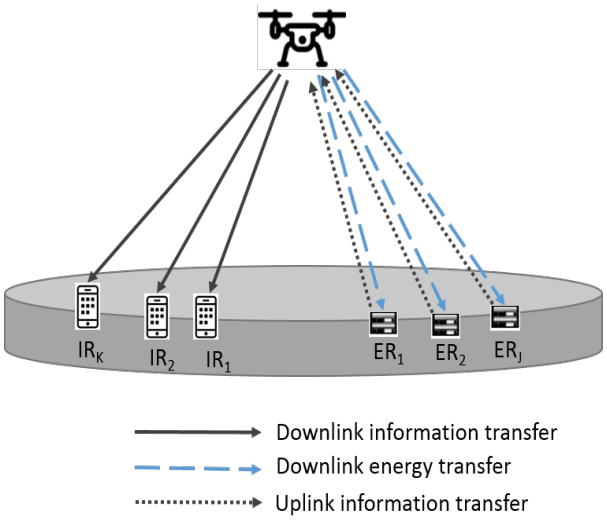

Fig. 1. System model.

in which f denotes the carrier frequency, c is the speed of light, and $\xi_{\text{LoS},j}$ and $\xi_{\text{NLoS},j}$ are the average environment-dependent excessive path losses in dB [11]. In (2), $p_{\text{LoS},j}$ denotes the probability that the UAV has LoS with ER_j [11], given by

$$p_{\text{LoS},j} = \frac{1}{1 + a\exp\left(-b\,\left(\frac{180}{\pi}\theta_j - a\right)\right)}, \tag{5}$$

where a and b are constant values related to the environment, and $\theta_j = \arccos(h_{\rm UAV}/d_j)$ is the elevation angle in radian between UAV and ER_j, with d_j being the Euclidean distance:

$$d_j = \sqrt{(X_{\rm UAV} - X_{\text{ER}_j})^2 + (Y_{\rm UAV} - Y_{\text{ER}_j})^2 + (h_{\rm UAV} - h_{\text{ER}_j})^2}. \tag{6}$$

The A2G channel model described above w.r.t. ERs ($\mathbf{g}$) applies to the IRs ($\mathbf{h}$) by replacing k with j and IR with ER in (1)-(6). For the channel between ER_j and UAV, $\mathbf{z}_j$, we also consider a Rician model as for $\mathbf{g}_j$, with $\mathbf{z}_j = \mathbf{z}'_j/\sqrt{L^{\rm U}_{\text{ER}_j}}$ and $L^{\rm U}_{\text{ER}_j}$ being the average G2A distance-dependent path-loss.

B. Energy Transmission

The UAV transmits energy signal $\mathbf{x}_1 \in \mathbb{C}^{N_E\times 1}$, which consists of J energy beams, one for each ER, i.e.,

$$\mathbf{x}_1 = \sum_{j=1}^{J}\sqrt{P^{\rm D}_j}\,\mathbf{w}_j s^{\rm ER}_j, \tag{7}$$

where $P^{\rm D}_j$ is the transmit power destined for ER_j, $s^{\rm ER}_j \in \mathcal{CN}(0,1)$ denotes the energy-carrying signal, and $\mathbf{w}_j \in \mathbb{C}^{N_E\times 1}$ is the corresponding energy beamforming vector. For the $j^{\rm th}$ ER, the received signal is given by

$$y^{\rm ER}_j = \mathbf{g}_j \sum_{i=1}^{J}\sqrt{P^{\rm D}_i}\,\mathbf{w}_i s^{\rm ER}_i + n^{\rm ER}_j, \tag{8}$$

where $n^{\rm ER}_j \sim \mathcal{CN}(0,\sigma^2)$ is the AWGN noise. Without loss of generality, we assume equal noise powers for all ERs, i.e., σ^2. It is assumed that the harvested energy is the result of the

energy signal, and that noise does not take part in it. Assuming the availability of perfect channel state information (CSI), the optimal weight vector $\mathbf{w}_j^\star$ is $\mathbf{g}_j^\dagger/\|\mathbf{g}_j\|$. Hence, energy that is harvested by ER_j during the first phase is given by

$$E_j = \zeta_j \alpha |\mathbf{g}_j \mathbf{w}_j^\star|^2 \sum_{i=1}^{J} \sqrt{P_i^{\mathrm{D}}} = \zeta_j \alpha \frac{\|\mathbf{g}_j'\|^2}{L_{\mathrm{ER}_j}^{\mathrm{D}}} P^{\mathrm{D}}, \quad (9)$$

where $0 < \zeta_j \leq 1$ is the energy-harvesting circuit efficiency [12], assumed the same for all ERs, and P^{D} is the total power destined to ERs.

C. Information Transmission

In the second phase, ERs use the harvested energy for their uplink communication with the UAV, simultaneously with the downlink transmission from the UAV to the IRs.

1) Uplink Information Transmission: The transmit power from the j^{th} ER is $P_j^{\mathrm{U}} = \frac{E_j}{1-\alpha}$. The UAV receives the superposed message signal of J ERs, and applies SIC to decode each device's message. The received signal at the UAV, $\mathbf{y}_{\mathrm{UAV}} \in \mathbb{C}^{N_E \times J}$, is given by

$$\mathbf{y}_{\mathrm{UAV}} = \sum_{j=1}^{J} \sqrt{P_j^{\mathrm{U}}}\, \mathbf{z}_j\, \mathbf{o}_j s_j^{\mathrm{UAV}} + \mathbf{H}_{\mathrm{SI}} \sum_{k=1}^{K} \sqrt{Q_k^{\mathrm{D}}}\, \mathbf{v}_k s_k^{\mathrm{IR}} + \mathbf{n}, \quad (10)$$

where $\mathbf{o}_j \in \mathbb{C}^{1\times N_E}$ is the beamforming vector of the j^{th} ER, and $s_j^{\mathrm{UAV}} \in \mathcal{CN}(0,1)$ is the normalized data symbol of ER_j towards the UAV. Further, $\mathbf{H}_{\mathrm{SI}} \in \mathbb{C}^{N_I \times N_E}$ is the self interference (SI) channel due to the simultaneous uplink and downlink processes [13], Q_k^{D} is the transmit power for IR_k, $\mathbf{v}_k \in \mathbb{C}^{N_I \times 1}$ is the corresponding beamforming vector, $s_k^{\mathrm{IR}} \in \mathcal{CN}(0,1)$ denotes the information-bearing signal for the k^{th} IR, and $\mathbf{n}$ is the AWGN with zero mean and covariance matrix $\mathbb{E}\{\mathbf{n}\mathbf{n}^\dagger\} = \sigma^2 \mathbf{I}_{N_E}$, where $\mathbf{I}$ is the identity matrix. We assume that powerful SI cancellation is in place [13], thus its effect can be ignored.

2) Downlink Information Transmission: The data signal $\mathbf{x}_2 \in \mathbb{C}^{N_I \times 1}$ sent by the UAV to the IRs consists of K information beams, one for each IR. Hence, we have

$$\mathbf{x}_2 = \sum_{k=1}^{K} \sqrt{Q_k^{\mathrm{D}}}\, \mathbf{v}_k s_k^{\mathrm{IR}}. \quad (11)$$

Each IR encounters interference from the uplink signals of ERs towards the UAV, as well as interference from the downlink beams to other IRs. The received signal at IR_k is given by

$$y_k^{\mathrm{IR}} = \mathbf{h}_k \sum_{i=1}^{K} \sqrt{Q_i^{\mathrm{D}}}\, \mathbf{v}_i s_i^{\mathrm{IR}} + \sum_{j=1}^{J} \sqrt{P_j^{\mathrm{U}}}\, \mathbf{o}_j s_j^{\mathrm{UAV}} + n_k^{\mathrm{IR}}. \quad (12)$$

Since the interferences from the ERs to IR_k are small compared to the interferences from other IRs, their effect can be neglected. Hence, the signal-to-interference-plus-noise ratio (SINR) at the k^{th} IR is formulated as

$$\gamma_k = \frac{Q_k^{\mathrm{D}} \mathbf{v}_k^H \mathbf{h}_k^H \mathbf{h}_k \mathbf{v}_k}{\sum\limits_{i=1, i\neq k}^{K} Q_i^{\mathrm{D}} \mathbf{v}_i^H \mathbf{h}_k^H \mathbf{h}_k \mathbf{v}_i + \sigma^2}, \quad \forall k. \quad (13)$$

III. Energy Efficiency Optimization

A. Energy Efficiency

Energy efficiency can be quantitatively measured by the bits of information reliably transferred to a receiver per unit of consumed energy at the transmitter [14]. To formulate the EE of the system under consideration, we have to construct the throughputs of the downlink and uplink stages. For the downlink information NOMA setup, where the channel gains of IRs are increasing when closer to the UAV (channel gain of IR_1 is larger than IR_2, and so on until IR_K), the rate in bps related to a given IR can be expressed as [14]:

$$R_k^{\mathrm{D}} = (1-\alpha) W \log_2 \left(1 + \frac{\frac{Q_k^{\mathrm{D}} \|\mathbf{h}_k'\|^2}{L_{\mathrm{IR}_k}^{\mathrm{D}}(1-\alpha)}}{\sum\limits_{i=1, i\neq k}^{K-1} \frac{Q_i^{\mathrm{D}} \|\mathbf{h}_k'\|^2}{L_{\mathrm{IR}_i}^{\mathrm{D}}(1-\alpha)} + 1} \right), \quad (14)$$

where W is the bandwidth. According to the principles of power-domain NOMA, for a given IR, the strong interfering signals are mainly due to the transmissions to users with low channel gains. The weakest channel user, IR_K, which receives low interferences due to the relatively low powers of the messages of high channel gain users, cannot cancel any interferences. However, the highest channel gain user, IR_1, which receives strong interferences due to the relatively high powers of the transmissions to weak users, can cancel all interfering signals [5]. On the other hand, for the uplink NOMA throughput, knowing that the channel gains are stronger when ERs are closer to the UAV (channel gain of ER_1 is larger than ER_2, and so on until ER_J), then based on (9) and (10), the rate related to a given ER can be expressed as [14]:

$$R_j^{\mathrm{U}} = (1-\alpha) W \log_2 \left(1 + \frac{\frac{\zeta P_j^{\mathrm{D}} \|\mathbf{g}_j'\|^2 \|\mathbf{z}_j'\|^2 \alpha}{L_{\mathrm{ER}_j}^{\mathrm{U}} L_{\mathrm{ER}_j}^{\mathrm{D}}(1-\alpha)}}{\sum\limits_{l=j+1}^{J} \frac{\zeta P_l^{\mathrm{D}} \|\mathbf{g}_l'\|^2 \|\mathbf{z}_l'\|^2 \alpha}{L_{\mathrm{ER}_l}^{\mathrm{U}} L_{\mathrm{ER}_l}^{\mathrm{D}}(1-\alpha)} + 1} \right). \quad (15)$$

The signal of the highest channel gain user, ER_1, is decoded first at the UAV. As a result, ER_1 experiences interference from all other ERs. Then, the signal for the second highest channel gain user is decoded until the last one, ER_J, [5].

Define the downlink throughput as the sum-rate of all IRs, i.e., $R^{\mathrm{D}} = \sum_{k=1}^{K} R_k^{\mathrm{D}}$, and the uplink throughput as the sum-rate $R^{\mathrm{U}} = \sum_{j=1}^{J} R_j^{\mathrm{U}}$. The EE of the system is expressed as

$$\eta = \frac{\text{Total Throughput}}{\text{Total Consumed Energy}} = \frac{R^{\mathrm{D}} + R^{\mathrm{U}}}{P_{\mathrm{DC}} + P^{\mathrm{D}} + Q^{\mathrm{D}}(1-\alpha)}, \quad (16)$$

where P_{DC} is the constant power consumption of the UAV, and where $P^{\mathrm{D}} = \sum_{j=1}^{J} P_j^{\mathrm{D}} = \beta P$ and $Q^{\mathrm{D}} = \sum_{k=1}^{K} Q_k^{\mathrm{D}} = (1-\beta)P$ are the powers dedicated to the ERs and the IRs, respectively, i.e., $P = P^{\mathrm{D}} + Q^{\mathrm{D}}$, where β indicates the percentage of power destined to ERs and $(1-\beta)$ indicates to the percentage of power destined to IRs. Hence, a larger value of β means that higher priority is given to the WPT.

IV. Energy Efficiency Maximization

The optimization problem which aims to maximize EE is formulated as follows:

$$\begin{aligned}
\mathrm{OP}_1: \quad & \max_{Q^{\mathrm{D}},P^{\mathrm{D}},\alpha,\beta} \quad \eta \\
& \text{subject to:} \quad P \le P_{\max}, \\
& \quad P_j^{\mathrm{U}} \le P_{j,\max}^{\mathrm{U}}, \quad \forall j, \\
& \quad \alpha < 1, \\
& \quad 0 \le \beta \le 1, \\
& \quad R_j^{\mathrm{U}} \ge R_{j,\min}^{\mathrm{U}}, \quad \forall j, \\
& \quad R_k^{\mathrm{D}} \ge R_{k,\min}^{\mathrm{D}}, \quad \forall k, \\
& \quad P_{\mathrm{thr}}^{\mathrm{U}} \le P_j^{\mathrm{U}} z_j - \sum_{l=j+1}^{J} P_l^{\mathrm{U}} z_l, \quad \forall j, \\
& \quad Q_{\mathrm{thr}}^{\mathrm{D}} \le \left(Q_k^{\mathrm{D}} - \sum_{m=1}^{k-1} Q_m^{\mathrm{D}} \right) h_{k-1}, \quad \forall k,
\end{aligned} \tag{17}$$

where $R_{j,\min}^{\mathrm{U}}$ and $R_{k,\min}^{\mathrm{D}}$ denote the minimum required rates of ER_j and IR_k, respectively, and where $P_{\mathrm{thr}}^{\mathrm{U}}$ and $Q_{\mathrm{thr}}^{\mathrm{D}}$ are the SIC detection thresholds of the uplink and downlink, respectively.

It is obvious that OP_1 is a fractional optimization problem with variables P^{D}, Q^{D}, and α, and is non-convex. Exploiting the idea in [15], the fractional programming problem can be transformed into a convex problem by introducing variable χ^* as the optimal EE when we have the optimal powers and optimal WPT fraction of time, α. Hereafter, for more tractability and to get a clearer insight into the system performance, we focus on the scenario with two ERs and two IRs. Accordingly, (17) becomes

$$\begin{aligned}
\mathrm{OP}_2: \quad & \max_{Q^{\mathrm{D}},P^{\mathrm{D}},\alpha,\beta} \quad \sum_{k=1}^{2} R_k^{\mathrm{D}} + \sum_{j=1}^{2} R_j^{\mathrm{U}} \\
& \quad - \chi^*(P_{DC} + P_D^{ER} + Q_D^{IR}(1-\alpha)) \\
& \text{subject to:} \quad P \le P_{\max}, \\
& \quad P_j^{\mathrm{U}} \le P_{j,\max}^{\mathrm{U}}, \quad j = 1,2, \\
& \quad \alpha < 1, \\
& \quad 0 \le \beta \le 1, \\
& \quad R_j^{\mathrm{U}} \ge R_{j,\min}^{\mathrm{U}}, \quad j = 1,2, \\
& \quad R_k^{\mathrm{D}} \ge R_{k,\min}^{\mathrm{D}}, \quad k = 1,2, \\
& \quad P_{\mathrm{thr}}^{\mathrm{U}} \le P_j^{\mathrm{U}} z_j - \sum_{l=j+1}^{J} P_l^{\mathrm{U}} z_l, j = 1,2, \\
& \quad Q_{\mathrm{thr}}^{\mathrm{D}} \le \left(Q_k^{\mathrm{D}} - \sum_{m=1}^{k-1} Q_m^{\mathrm{D}} \right) h_{k-1}, k = 1,2.
\end{aligned} \tag{18}$$

By introducing $\vartheta \ge 0$, $\varsigma_1 \ge 0$, $\varsigma_2 \ge 0$, $\varepsilon \ge 0$, $\varrho \ge 0$, $\varphi_1 \ge 0$, $\varphi_2 \ge 0$, $\lambda_1 \ge 0$, $\lambda_2 \ge 0$, $\mu \ge 0$, and $\phi \ge 0$, as the Lagrange multipliers associated with the constraints in OP_2, the Lagrangian function of OP_2 can be formulated as:

$$\begin{aligned}
& \mathcal{L}(\vartheta, \varsigma_1, \varsigma_2, \varepsilon, \varrho, \varphi_1, \varphi_2, \lambda_1, \lambda_2, \mu, \phi, \beta, Q_1^{\mathrm{D}}, Q_2^{\mathrm{D}}, P_1^{\mathrm{D}}, P_2^{\mathrm{D}}, \alpha) \\
& = \sum_{k=1}^{2} R_k^{\mathrm{D}} + \sum_{j=1}^{2} R_j^{\mathrm{U}} - \chi^*(P_{\mathrm{DC}} + \beta P + (1-\beta)(1-\alpha)P) \\
& - \vartheta(P - P_{\max}) - \varsigma_1(P_1^{\mathrm{U}} - P_{1,\max}^{\mathrm{U}}) - \varsigma_2(P_2^{\mathrm{U}} - P_{2,\max}^{\mathrm{U}}) \\
& - \varepsilon(\alpha - 1) - \varphi_1(R_{1,\min}^{\mathrm{U}} - R_1^{\mathrm{U}}) - \varphi_2(R_{2,\min}^{\mathrm{U}} - R_2^{\mathrm{U}}) \\
& - \varrho(\beta - 1) - \lambda_1(R_{1,\min}^{\mathrm{D}} - R_1^{\mathrm{D}}) - \lambda_2(R_{2,\min}^{\mathrm{D}} - R_2^{\mathrm{D}}) \\
& - \mu(P_{\mathrm{thr}}^{\mathrm{U}} - P_1^{\mathrm{U}} z_1 + P_2^{\mathrm{U}} z_2) - \phi(Q_{\mathrm{thr}}^{\mathrm{D}} - Q_2^{\mathrm{D}} h_1 + Q_1^{\mathrm{D}} h_1).
\end{aligned} \tag{19}$$

We assume that the UAV uses its maximum power, such that $\beta P_{\max} = P^{\mathrm{D}}$ and $(1-\beta)P_{\max} = Q^{\mathrm{D}}$. Our goal is to find β, Q_1^{D}, and hence $Q_2^{\mathrm{D}} = (1-\beta)P_{\max} - Q_1^{\mathrm{D}}$, as well as P_1^{D} which also implicitly means $P_2^{\mathrm{D}} = \beta P_{\max} - P_1^{\mathrm{D}}$, and the optimal WPT fraction of time (α^*). The optimization problem OP_2 is split into two stages. In the first stage, the aim is to determine the optimized value of β. In the second stage, the optimization problem OP_2 after obtaining β is split into two sub-problems. The first one corresponds to the downlink WIT, where the purpose is to find Q_1^{D} and Q_2^{D}, taking into account that the WIT takes place in the second phase of the process, with the constraints focused on the first, fifth, and eighth constraints of OP_2. In the second sub-problem, the aim is to optimize P_1^{D}, P_2^{D}, and α, where this accounts for the first, second, third, fifth, and seventh constraints. After getting the optimized parameters, we merge them together to find the optimized EE, which is the result of the optimized rates on both processes. Taking into account that OP_2 is a nonlinear programming problem, this can be done through derivation of the Lagrangian function (19) w.r.t. Q_1^{D}, P_1^{D}, and α, and setting them to zero, i.e.,

$$\frac{\partial \mathcal{L}}{\partial Q_1^{\mathrm{D}}} = 0, \quad \frac{\partial \mathcal{L}}{\partial P_1^{\mathrm{D}}} = 0, \quad \frac{\partial \mathcal{L}}{\partial \alpha} = 0, \tag{20}$$

where we dropped the arguments of the functional $\mathcal{L}(\vartheta, \varsigma_1, \varsigma_2, \varepsilon, \varrho, \varphi_1, \varphi_2, \lambda_1, \lambda_2, \mu, \phi, \beta, Q_1^{\mathrm{D}}, Q_2^{\mathrm{D}}, P_1^{\mathrm{D}}, P_2^{\mathrm{D}}, \alpha)$ for notational simplicity. The updating of the Lagrangian variables (ϑ, ς_1, ς_2, ε,ϱ, φ_1, φ_2, λ_1, λ_2 , μ, and ϕ) can be done using the gradient-decent method, according to

$$\vartheta(i+1) = [\vartheta(i) - \triangle_{\vartheta}(P_{\max} - P)]^+, \tag{21}$$

$$\varsigma_1(i+1) = [\varsigma_1(i) - \triangle_{\varsigma_1}(P_{1,\max}^{\mathrm{U}} - P_1^{\mathrm{U}})]^+, \tag{22}$$

$$\varsigma_2(i+1) = [\varsigma_2(i) - \triangle_{\varsigma_2}(P_{2,\max}^{\mathrm{U}} - P_2^{\mathrm{U}})]^+, \tag{23}$$

$$\varepsilon(i+1) = [\varepsilon(i) - \triangle_{\varepsilon}(1-\alpha)]^+, \tag{24}$$

$$\varrho(i+1) = [\varrho(i) - \triangle_{\varrho}(1-\beta)]^+, \tag{25}$$

$$\varphi_1(i+1) = [\varphi_1(i) - \triangle_{\varphi_1}(R_1^{\mathrm{U}} - R_{1,\min}^{\mathrm{U}})]^+, \tag{26}$$

$$\varphi_2(i+1) = [\varphi_2(i) - \triangle_{\varphi_2}(R_2^{\mathrm{U}} - R_{2,\min}^{\mathrm{U}})]^+, \tag{27}$$

$$\lambda_1(i+1) = [\lambda_1(i) - \triangle_{\lambda_1}(R_1^{\mathrm{D}} - R_{1,\min}^{\mathrm{D}})]^+, \tag{28}$$

$$\lambda_2(i+1) = [\lambda_2(i) - \triangle_{\lambda_2}(R_2^{\mathrm{D}} - R_{2,\min}^{\mathrm{D}})]^+, \tag{29}$$

$$\mu(i+1) = [\mu(i) - \triangle_{\mu}(P_1^{\mathrm{U}} z_1 - P_2^{\mathrm{U}} z_2 - P_{\mathrm{thr}}^{\mathrm{U}})]^{+}, \quad (30)$$

$$\phi(i+1) = [\phi(i) - \triangle_{\phi}(Q_2^{\mathrm{D}} h_1 + Q_1^{\mathrm{D}} h_1 - Q_{\mathrm{thr}}^{\mathrm{D}})]^{+}, \quad (31)$$

where i is the iteration index, and the $\triangle$'s are the iteration steps.

The closed form of the optimized power fraction can be obtained by solving $\frac{\partial \mathcal{L}}{\partial \beta} = 0$, which leads to:

$$\beta = \frac{\alpha\varphi_1 + \alpha}{\alpha\varphi_1 + \alpha\lambda_1 + 2\alpha} + \frac{((1-\alpha)\varphi_1 - \alpha + 1)L_{\mathrm{IR}_1}^{\mathrm{D}}}{(\alpha\varphi_1 + \alpha\lambda_1 + 2\alpha)\|\mathbf{h}_I{}'\|^2 P_{\max}} + \frac{((\alpha-1)\lambda_1 + \alpha - 1)L_{\mathrm{ER}_1}^{\mathrm{D}} L_{\mathrm{ER}_1}^{\mathrm{U}}}{(\alpha\varphi_1 + \alpha\lambda_1 + 2\alpha)\|\mathbf{g}_I{}'\|^2\|\mathbf{z}_I{}'\|^2 P_{\max}\zeta} - \chi^* \alpha P_{\max} - \varrho - \frac{\zeta\alpha\|\mathbf{g}_I{}'\|^2 P_{\max}}{L_{\mathrm{ER}_1}^{\mathrm{D}}(1-\alpha)}. \quad (32)$$

The solution of the optimization problem OP_2 is summarized in Algorithm 1, where $Q_{1_0}^{\mathrm{D}}$, $P_{1_0}^{\mathrm{D}}$, and α_0 denote the initial values for Q_1^{D}, P_1^{D}, and α, respectively.

Algorithm 1 Energy-Efficient Resource Allocation

Input: $(X_{\mathrm{UAV}}, Y_{\mathrm{UAV}}, h_{\mathrm{UAV}})$; $(X_{\mathrm{ER}_j}, Y_{\mathrm{ER}_j}, h_{\mathrm{ER}_j})$, $j = 1, 2$; $(X_{\mathrm{IR}_k}, Y_{\mathrm{IR}_k}, h_{\mathrm{IR}_k})$, $k = 1, 2$; a, b, β, ξ_{LoS}, ξ_{NLoS}, f, η, σ, $R_{\min}^{\mathrm{U}}$, $R_{\min}^{\mathrm{D}}$, $\triangle_{\varsigma_1}$, $\triangle_{\varsigma_2}$, $\triangle_{\varepsilon}$, $\triangle_{\varrho}$, $\triangle_{\varphi_1}$, $\triangle_{\varphi_2}$, $\triangle_{\lambda_1}$, $\triangle_{\lambda_2}$, $\triangle_{\mu}$, $\triangle_{\phi}$, and χ^*.

Output: $\left[\beta, Q_1^{\mathrm{D}}, Q_2^{\mathrm{D}}, P_1^{\mathrm{D}}, P_2^{\mathrm{D}}, \alpha\right]$.

Initialization: $\left[Q_{1_0}^{\mathrm{D}}, P_{1_0}^{\mathrm{D}}, \alpha_0\right]$, $\vartheta = 0$, $\varsigma_1 = 0$, $\varsigma_2 = 0$, $\varepsilon = 0$, $\varphi_1 = 0$, $\varphi_2 = 0$, $\lambda_1 = 0$, $\lambda_2 = 0$, $\mu = 0$, $\phi = 0$.

1: Calculate β as per (32).
2: Update ϑ, λ_1, λ_2 and ϕ based on (21), (28), (29), and (31), respectively.
3: Solve (20) to obtain Q_1^{D}.
4: Update ϑ, ς_1, ς_2, ε, φ_1, φ_2, and μ based on (21), (22), (23), (24), (26), (27), and (30), respectively.
5: Solve (20) to obtain P_1^{D} and α.
6: Compute $\left[Q_1^{\mathrm{D}*}, Q_2^{\mathrm{D}*}, P_1^{\mathrm{D}*}, P_2^{\mathrm{D}*}, \alpha^*\right]$ by solving (18).

V. Numerical Results and Discussion

In the simulations, we set $a = 9.6$, $b = 0.28$, $\xi_{\mathrm{LoS}} = 1$ dB, $\xi_{\mathrm{NLoS}} = 20$ dB, $f = 2$ GHz, $W = 200$ kHz, $\eta = 0.8$, $\sigma^2 = 1$, and $N_E = N_I = 2$. The position of ER_1 is fixed at (1,0,0), and we vary the horizontal coordinate of ER_2 (x,0,0). The UAV is positioned at (0,0,10). Also, the position of IR_1 is set to (-1,0,0), and we vary the horizontal coordinate of IR_2 (-x,0,0). We set $Q_{\mathrm{thr}}^{\mathrm{D}} = P_{\mathrm{thr}}^{\mathrm{U}} = 0.05$ Watt, $P_{\mathrm{DC}} = 5$ Watt, $P_{\max} = 3$ Watt, and $R_{\min}^{\mathrm{U}} = R_{\min}^{\mathrm{D}} = 12$ Kbps.

As a first stage of the process, β is determined before starting the actual transmissions towards the ERs and IRs. According to the closed-form expression of β along with the symmetrical positions of ERs and IRs in our setup, the power among ERs and IRs is split equally. Once β is obtained, the transmissions towards the ERs and IRs start. Fig. 2 shows the throughput of each IR along with the summation of those rates. It is clear that the throughput of IR_1 always outperforms that of IR_2, for both the OMA and NOMA schemes. With

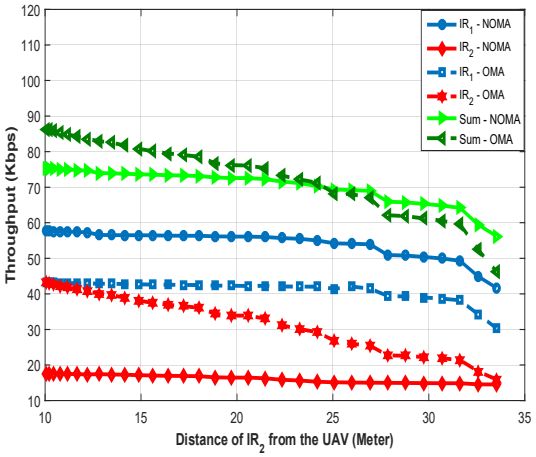

Fig. 2. Downlink throughput.

OMA protocol, the UAV sends the information separately by dedicating half of the transmission phase, $(1-\alpha)/2$, to each IR. The sum-rate with OMA is better than with NOMA for small distances of IR_2 w.r.t. the UAV, while NOMA starts to outperform OMA as the said distance increases and the link of IR_2 becomes much weaker compared to the link of the strong user.

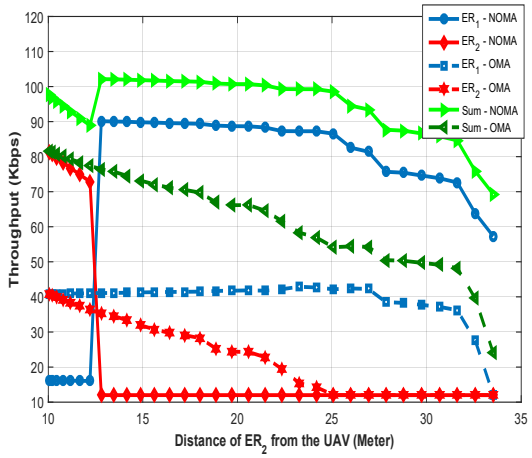

Fig. 3. Uplink throughput.

Energy harvested by the ERs from the downlink WPT is used for their NOMA uplink communication with the UAV. Figure 3 illustrates the throughput of each ER along with the sum-rate. Results of conventional uplink OMA, where each ER sends its information to the UAV during half of the second phase, i.e., $(1-\alpha)/2$, are also provided. It is obvious that the throughput of ER_1 mostly outperforms the throughput of ER_2 in the OMA set-up. With NOMA, there are some variation and correlation between the rates of ER_1 and ER_2. As observed, the throughput of ER_1 decreases sharply when ER_2 becomes closer to the UAV, which implicitly means that its transmission increases the interference on the ER_1 signal. This can be clearly noticed when the distance of ER_2 is less than 13 meters, which means that it starts to have a strong connection with the UAV. In both OMA and NOMA schemes, the rate of ER_1 starts to decrease when the distance of ER_2

from the UAV increases, which is due to the minimum rate constraints in both schemes. As the rate of ER_2 must also satisfy the said constraints, and with decreasing channel gain with the distance, this is compensated by specifying more power towards ER_2 on the account of ER_1 in both OMA and NOMA. It is clear that the sum-rate of the NOMA based uplink is larger compared to OMA, due to the simultaneous transmissions from the ERs.

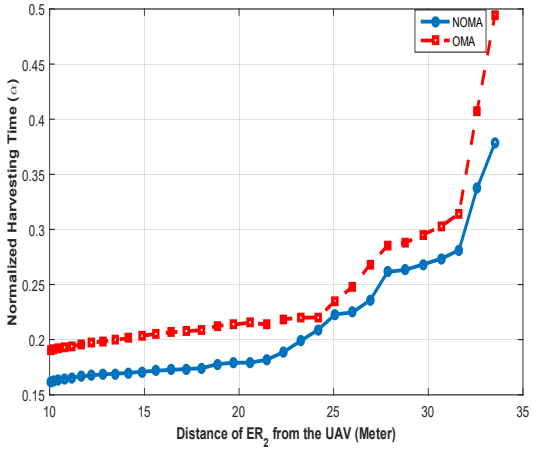

Fig. 4. Normalized harvesting time.

Figure 4 shows the optimal normalized harvesting time, α^*, for different positions of ER_2, while the position of ER_1 remains fixed. The figure compares the fraction of time slot needed for the WPT to ERs to enable their uplink transmissions using NOMA or OMA. As observed, in all cases, the WPT time in the NOMA case is lower compared to OMA.

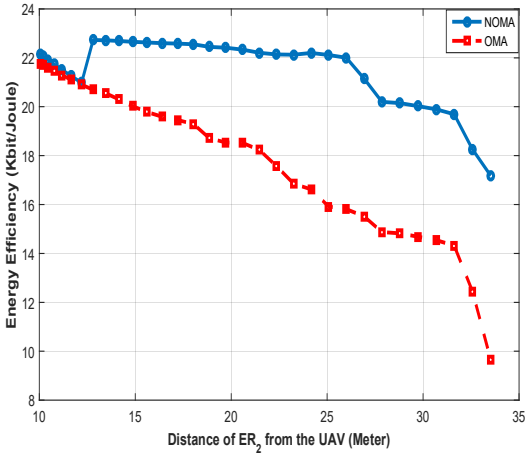

Fig. 5. System energy efficiency.

Figure 5 compares the effect of different access schemes, i.e., NOMA and OMA, on the EE of the system. Results are plotted as a function of the distance of ER_2 from the UAV, taking into account that the downlink throughput of IR_2 is constructed from the same distance of the uplink throughput of ER_2. The EE with the NOMA scheme is considerably better than that with OMA for different distances of ER_2 w.r.t the UAV, and the difference increases as the distance of ER_2 from the UAV increases. It is important to note that when the said distance is small and that the ERs and IRs are close to each other, then OMA and NOMA yield similar performance, due to the loss of the required distinctions between users in NOMA.

VI. Conclusion

We investigated the resource allocation in a multiple-antenna UAV deployed for transmitting data to information receivers, as well as wireless power to energy receivers to assist their uplink data communication towards it through NOMA protocol. The resource allocation problem was solved by optimizing the transmit powers towards maximization of the energy efficiency (EE). The results showed that significant EE can be achieved by the proposed allocation. In particular, it was shown that EE of the NOMA-based system outperforms that of OMA in most cases w.r.t. the position of the weak user, and that reduced WPT time is needed at the UAV to power devices when NOMA is used for the data communication. Current investigations include generalization of the solution for high node densities and UAV trajectory optimization.

References

[1] A. Merwaday and I. Guvenc, "UAV assisted heterogeneous networks for public safety communications," in *Proc. IEEE Wireless Commun. and Netw. Conf. Workshops (WCNC)*, 2015, pp. 329–334.

[2] X. Zhou, R. Zhang, and C. K. Ho, "Wireless information and power transfer: Architecture design and rate-energy tradeoff," in *Proc. IEEE Global Commun. Conf. (GC)*, 2012, pp. 3982–3987.

[3] S. Najmeddin, A. Bayat, S. Aïssa, and S. Tahar, "Energy-efficient resource allocation for UAV-enabled wireless powered communications," in *Proc. IEEE Wireless Commun. and Netw. Conf. (WCNC)*, 2019, pp. 1–6.

[4] F. Huang, J. Chen, H. Wang, G. Ding, Z. Xue, Y. Yang, and F. Song, "UAV-assisted SWIPT in internet of things with power splitting: Trajectory design and power allocation," *IEEE Access*, vol. 7, pp. 68 260–68 270, 2019.

[5] M. S. Ali, H. Tabassum, and E. Hossain, "Dynamic user clustering and power allocation for uplink and downlink non-orthogonal multiple access (NOMA) systems," *IEEE Access*, vol. 4, pp. 6325–6343, 2016.

[6] M. F. Sohail, C. Y. Leow, and S. Won, "Non-orthogonal multiple access for unmanned aerial vehicle assisted communication," *IEEE Access*, vol. 6, pp. 22 716–22 727, 2018.

[7] P. K. Sharma and D. I. Kim, "UAV-enabled downlink wireless system with non-orthogonal multiple access," in *Proc. IEEE Global Commun. Conf. Workshops (GC Wkshps)*, 2017, pp. 1–6.

[8] W. Mei and R. Zhang, "Uplink cooperative NOMA for cellular-connected UAV," *IEEE J. Sel. Topics Signal Process.*, vol. 13, no. 3, pp. 644–656, June 2019.

[9] J. Xu, Y. Zeng, and R. Zhang, "UAV-enabled wireless power transfer: Trajectory design and energy optimization," *IEEE Trans. Wireless Commun.*, vol. 17, no. 8, pp. 5092–5106, Aug. 2018.

[10] S. Jeong, O. Simeone, and J. Kang, "Mobile edge computing via a UAV-mounted cloudlet: Optimization of bit allocation and path planning," *IEEE Trans. Veh. Technol.*, vol. 67, no. 3, pp. 2049–2063, Mar. 2018.

[11] A. Al-Hourani, S. Kandeepan, and S. Lardner, "Optimal LAP altitude for maximum coverage," *IEEE Wireless Commun. Lett.*, vol. 3, no. 6, pp. 569–572, Dec. 2014.

[12] M. Xia and S. Aïssa, "On the efficiency of far-field wireless power transfer," *IEEE Trans. Signal Process.*, vol. 63, no. 11, pp. 2835–2847, Jun. 2015.

[13] T. Riihonen, S. Werner, and R. Wichman, "Mitigation of loopback self-interference in full-duplex MIMO relays," *IEEE Trans. Signal Process.*, vol. 59, no. 12, pp. 5983–5993, Dec. 2011.

[14] T. A. Zewde and M. C. Gursoy, "NOMA-based energy-efficient wireless powered communications," *IEEE Trans. Green Commun. Netw.*, vol. 2, no. 3, pp. 679–692, Sep. 2018.

[15] D. W. K. Ng, E. S. Lo, and R. Schober, "Energy-efficient resource allocation for secure OFDMA systems," *IEEE Trans. Veh. Technol.*, vol. 61, no. 6, pp. 2572–2585, Jul. 2012.